Atmos. Chem. Phys. Discuss., 13, 22025–22058, 2013
www.atmos-chem-phys-discuss.net/13/22025/2013/
doi:10.5194/acpd-13-22025-2013

Atmospheric Chemistry and Physics
Discussions
Open Access

Summertime free tropospheric ozone pool over the Eastern Mediterranean/Middle East

P. Zanis[1], P. Hadjinicolaou[2], A. Pozzer[3], E. Tyrlis[2], S. Dafka[1,4], N. Mihalopoulos[2,5], and J. Lelieveld[2,3]

[1]Department of Meteorology and Climatology, School of Geology, Aristotle University of Thessaloniki, University Campus, Thessaloniki, Greece
[2]Energy, Environment and Water Research Center, The Cyprus Institute, Nicosia, Cyprus
[3]Max Planck Institute for Chemistry, Mainz, Germany
[4]Climatology, Climate Dynamics and Climate Change, Department of Geography, Justus-Liebig University of Giessen, Germany
[5]Environmental Chemical Processes Laboratory, Department of Chemistry, University of Crete, Heraklion, Greece

Received: 23 May 2013 – Accepted: 6 August 2013 – Published: 23 August 2013

Correspondence to: P. Zanis (zanis@geo.auth.gr)

Published by Copernicus Publications on behalf of the European Geosciences Union.

Abstract

Observations show that the Mediterranean troposphere is characterized by a marked enhancement in summertime ozone with a maximum over the Eastern Mediterranean. This has been linked to enhanced ozone photochemical production and subsidence under cloud-free anticyclonic conditions. The Eastern Mediterranean region has among the highest levels of background tropospheric ozone around the globe and it can be considered as a global air pollution hotspot. A 12 yr climatological analysis (1998–2009) of free tropospheric ozone was carried out over the region based on ECMWF (European Centre for Medium-Range Weather Forecasts) ERA-interim reanalysis data and simulations with the EMAC (ECHAM5-MESSy for Atmospheric Chemistry) atmospheric chemistry climate model. EMAC is nudged towards the ECMWF analysis data and includes a stratospheric ozone tracer. A characteristic summertime pool with high ozone concentrations is found in the middle troposphere over the Eastern Mediterranean/Middle East (EMME) by ERA-interim ozone data, which is supported by Tropospheric Emission Spectrometer (TES) satellite ozone data and simulations with EMAC. The enhanced ozone over the EMME is a robust feature, propagating down to lower free tropospheric levels. The investigation of ozone in relation to potential vorticity and water vapour and the stratospheric ozone tracer indicates that the dominant mechanism causing the free tropospheric ozone pool is downward transport from the upper troposphere and lower stratosphere associated with the enhanced subsidence and the limited outflow transport that dominates the summertime EMME circulation. The implications of these summertime high free tropospheric ozone values on the seasonal cycle of near surface ozone over the Mediterranean are discussed.

1 Introduction

Ozone is central in the control of the oxidizing capacity of the troposphere (Chameides and Walker, 1973; Crutzen,1988; Penkett, 1988). Furthermore ozone is a greenhouse gas and its increase causes a radiative forcing leading to warming at the Earth's surface (IPCC, 2007). Ozone in the free troposphere has a longer lifetime compared to the boundary layer, which enables transport on regional to hemispheric scales and it has a proportionally greater influence on climate than ozone near the surface (Lacis et al., 1990). The main sources of tropospheric ozone are photochemical production through oxidation of VOCs (volatile organic compounds) and CO in the presence of NO_x and stratosphere-to-troposphere transport (e.g. Lelieveld and Dentener, 2000). Nowadays, there is broad agreement that photochemistry is the major contributor to the observed background ozone levels in the troposphere (Crutzen et al., 1999; Lelieveld and Dentener, 2000). Nevertheless, stratosphere-to-troposphere transport (STT) can be important in the middle and upper troposphere in regions where meteorological conditions favour downward transport, and in cases of deep stratospheric intrusions reaching into the lower troposphere (Roelofs and Lelieveld, 1997; Sprenger and Wernli, 2003; Akritidis et al., 2010).

In the Eastern Mediterranean (EM) during summer, comparatively highest levels of lower tropospheric ozone are found and the region is considered to be a global air pollution hotspot owing to the cloud-free conditions and high solar radiation intensity and because it is at the crossroads of polluted air masses from Europe, Africa and Asia (Zerefos et al., 2002; Lelieveld et al., 2002; Kanakidou et al., 2011). Furthermore, EM is also favorable to deep STT events because it lies southwards of the typical position of the polar front jet at the ending point of a pathway characteristic of stratospheric intrusions (Galani et al., 2003; Sprenger and Wernli, 2003).

These high ozone levels have the potential to strongly impact regional air quality and radiative forcing. The EU air quality standard for human health protection is often exceeded during summer, as shown by measurements at rural and baseline stations located upwind of urban areas (Kourtidis et al., 1996; Kalabokas and Bartzis, 1998; Kalabokas et al., 2000; Kouvarakis et al., 2000; Kalabokas and Repapis, 2004; Gerasopoulos et al., 2005) as well as measurements during campaigns over the Aegean (Kourtidis et al., 2002; Kouvarakis et al., 2002). Recently, Richards et al. (2013) showed that both the Tropospheric Emission Spectrometer (TES) and the Global Ozone Monitoring Experiment-2 (GOME-2) satellite instruments were able to detect enhanced levels of ozone in the lower troposphere over the Mediterranean region during the summer. Results from Chemistry Transport Models (CTMs) indicate that the largest portion of this high ozone over EM is beyond local emission controls (Zerefos et al., 2002) and that ozone in the lower troposphere originates mainly from the European continent (Roelofs et al., 2003). Biogenic emissions in summer may also impact the ozone levels in the lower troposphere of the Mediterranean Basin (Liakakou et al., 2007; Richards et al., 2013), being very sensitive to temperature changes (Im et al., 2011).

An important meteorological factor associated with these high surface and boundary layer ozone levels in summer is the anticyclonic flow and associated high pressures over the Central Mediterranean and the Balkans leading to enhanced photochemical ozone production but also tropospheric subsidence (Kalabokas et al., 2008). Another important factor is long-range transport of air masses from northern directions, rich in ozone and ozone precursors, passing over the sunlit Eastern Mediterranean, especially through the Aegean channel, together with emissions from local sources (Zerefos et al., 2002; Kouvarakis et al., 2002; Kalabokas et al., 2007). The Etesian wind system, which is the dominant flow regime during summer and early autumn over the Aegean Sea and EM, with persistent northerly winds in the lower troposphere, sets up the typical transport regime (Repapis, 1977; Kallos et al., 1998; Poupkou et al., 2011; Anagnostopoulou et al., 2013). Recently, Kalabokas et al. (2013) concluded that the highest ozone concentrations in the lower troposphere over EM and subsequently in the boundary layer are associated with large scale subsidence from the upper troposphere, which is a characteristic feature of the EM summer circulation inhibiting cloud formation and convection. The dynamics of Etesians are tightly interwoven with the large scale subsidence observed over the EM and both are interconnected manifestations of the remote South Asian Monsoon forcing (Rodwell and Hoskins, 1996, 2001; Ziv et al., 2004; Tyrlis et al., 2012). Essentially the monsoon regulates the seasonal cycle of the summer EM circulation, while the shorter term variability is controlled by the mid-latitude dynamics and features alternating phases of enhanced northerly flow (Etesian outbreaks) interrupted by quiet spells (Tyrlis et al., 2013).

There are also a number of studies reporting high ozone values in the middle and upper troposphere which extend to larger geographical areas over the Eastern Mediterranean and Middle East. Already in earlier observational studies, vertical profiles from the MOZAIC program on commercial aircraft indicated high summer mixing ratios over the area (Marenco et al., 1998; Stohl et al., 2001). Modeling studies showed high ozone values at 500 hPa over the Middle East in July (Jonson et al., 2001; Li et al., 2001). Li et al. (2001) simulated with a CTM a summertime ozone maximum over the Middle East, with mean mixing ratios in the middle and upper troposphere in excess of 80 ppbv being consistent with the few observations from commercial aircraft in the region. Roelofs et al. (2003) reported a layer of 4–6 km thickness over the region with up to 120 ppbv of ozone based on both observations and model simulations.

An important dynamical mechanism controlling the chemical composition of the middle and upper troposphere over the area is an inherent feature of the Indian summer monsoon, the Tropical Easterly Jet (TEJ) stream, a belt of strong easterly winds, which transports air from Asia over North Africa between 200 and 100 hPa and, aided by the upper tropospheric anticyclone over the Arabian Peninsula, toward the Eastern Mediterranean (Scheeren et al., 2003). Li et al. (2001) concluded that the anticyclonic circulation in the middle and upper troposphere over the Middle East funnels northern midlatitude pollution, transported in the westerly subtropical jet as well as lightning NO_x from the Indian monsoon and pollution from eastern Asia transported in the TEJ. Recently, Richards et al. (2013) performed CTM simulations and found that in the mid and upper troposphere almost all ozone originates from long-range transport, with the Asian monsoon outflow having the greatest impact.

On the other hand, there are contradicting results regarding the impact of STT on these high ozone levels in the middle and upper troposphere. For example, Li et al. (2001) reported that transport from the stratosphere does not contribute significantly to these high ozone levels while Roelofs et al. (2003) found substantial contribu-

Title Page
Abstract Introduction
Conclusions References
Tables Figures
◀| |▶
◀ ▶
Back Close
Full Screen / Esc
Printer-friendly Version
Interactive Discussion

tions by transport from the stratosphere. Also, a study of Stratosphere–Troposphere Exchange (STE) over the Eastern Mediterranean indicated that cross-tropopause transport can be intense, related to the distinct summertime meteorological conditions over South Asia and the Arabian Peninsula (Traub and Lelieveld, 2003). Recently, Lelieveld et al. (2009) linked the summertime high middle-troposphere ozone levels over Middle East to severe near surface ozone air pollution in the Persian Gulf region, pointing also the important contribution of stratospheric ozone.

The aim of this work is to investigate the role and the contribution of the controlling transport mechanisms for the characteristic summertime pool with high ozone concentrations in the middle troposphere over EMME area propagating down to lower free tropospheric levels and the implications for near surface ozone at the Mediterranean Basin.

2 Data and EMAC model description

2.1 ERA-interim data

ERA-Interim is the latest global atmospheric reanalysis produced by the European Centre for Medium-Range Weather Forecasts (ECMWF) covering the period from 1 January 1979 onwards, and has been continued to the present (Dee et al., 2011). The ERA-Interim atmospheric model and reanalysis system is configured with following spatial resolution: 60 levels in the vertical, with the top level at 0.1 hPa; T255 spherical-harmonic representation for the basic dynamical fields; a reduced Gaussian grid with approximately uniform 79 km spacing for surface and other grid-point fields (Berrisford et al., 2011). Information about the current status of ERA-Interim production, availability of data online, and near-real-time updates of various climate indicators derived from ERA-Interim data, can be found at http://www.ecmwf.int/research/era.

Focusing on the ozone product, Dethof and Hólm (2004) have described in detail the main characteristics the ECMWF ozone system of the ERA-40 reanalysis project.

As pointed out by Dethof and Hólm (2004), the ozone first guess used at ECMWF is derived from an updated version of the Cariolle and Déqué (1986) scheme. In this scheme, the ozone continuity equation is expressed as a linear relaxation towards a photochemical equilibrium for the local value of the ozone mixing ratio, the temperature, and the overhead ozone column. An additional ozone destruction term is used to parameterize the heterogeneous chemistry as a function of the equivalent chlorine content for the actual year. Most of that discussion still applies to ERA-Interim, although a number of changes and improvements were implemented in the latest reanalysis project. Description of the implemented scheme improvements can be found in Cariolle and Teyssédre (2007).It should be also noted that the ozone data assimilated in ERA-Interim uses a larger dataset than was used for ERA-40, for example the Global Ozone Monitoring Experiment (GOME) ozone profiles (Dragani, 2011). Dragani (2011) carried out a quality assessment of the ERA-interim ozone product, basically for the stratospheric levels and the mean total column ozone (TCO), showing generally consistent results when compared with ozone retrievals from a number of satellite instruments. The ERA-interim data used in the current analysis include monthly mean values of ozone, potential vorticity, specific humidity and the three components of the wind (u, v, and w) at 27 pressure levels from 1000 hPa up to 100 hPa for the period 1998–2009.

2.2 TES and EMEP ozone data

The Tropospheric Emission Spectrometer (TES) on the Earth Observing System (EOS) Aura mission is a high-resolution infrared imaging Fourier transform spectrometer covering the spectral range 650–3050 cm (3.3–15.4 m) at a spectral resolution of 0.1 cm^{-1} (nadir viewing) or 0.025 cm^{-1} (limb viewing). The major aim is to determine the chemical state of the Earth's troposphere (extending from the surface to about 10–15 km altitude). In particular, TES produces vertical profiles 0–32 km of important pollutant and greenhouse gases such as carbon monoxide, ozone, methane, and water vapor on a global scale every other day. Moreover, the TES investigation is especially focused on mapping the global distribution of tropospheric ozone and on understanding the factors that control ozone concentrations (Beer et al., 2001; Beer, 2006).The TES data used in the current analysis include daily (profile nadir) mean values of ozone for the period 2005–2009.

Furthermore in our analysis we considered near surface ozone data from four baseline maritime ozone stations in the Mediterranean Basin (see Fig. 1) from the EMEP (European Monitoring and Evaluation Programme) network at: (a) Cabo de Creus, Spain (ES10, 42.32° N, 3.32° E), (b) Giordan Lighthouse – Gozo, Malta (MT01, 36.07° N, 14.22° E), (c) Finokalia – Crete, Greece (GR02, 35.32° N, 25.67° E) and (d) Ag. Marina, Cyprus (CY02, 35.07° N, 33.12° E). The stations MT01, GR02 and CY02 started operation in 1997 while ES10 in 1999.

2.3 EMAC model description and set-up

The data used in this study are from a simulation with the ECHAM5/MESSy for Atmospheric Chemistry (EMAC) model, comprising the 5th generation European Centre – Hamburg general circulation model (GCM), ECHAM5 (Roeckner et al., 2006) coupled to the Modular Earth Submodel System, MESSy (Jöckel et al., 2005). The EMAC modelling system represents emissions, multiphase reactions, deposition and transport of chemical species, as well as radiation, cloud and dynamical processes from the surface up to the mesosphere. The modelled ozone data used in this study are taken from the EMAC version 2 run (Jöckel et al., 2010), based on an extensive evaluated version of the model (Joeckel et al., 2006; Pozzer et al., 2007). The model has a horizontal resolution of around 2.8 ° in longitude and latitude (T42 in spectral truncation). In the vertical direction the model has 90 layers from the ground to 0.01 hPa, 19 of which lie between the middle troposphere and the lower stratosphere (approx. between 500 hPa and 100 hPa) and resolving adequately the region around the tropopause, allowing for realistic stratosphere-troposphere interactions (Lelieveld et al., 2007). The model run was originally covering the period 1998–2008 but the simulation was further extended for an additional year, i.e. until end of 2009. The simulation was nudged towards the actual tropospheric meteorology (excluding the boundary layer and up to 100 hPa), with temperature, surface pressure, divergence and vorticity data from the operational forecast analyses of the European Centre for Medium-Range Weather Forecasts (ECMWF).

The chemical mechanism includes 110 species and a total of 286 gas phase, heterogeneous and liquid phase reactions (Sander et al.; 2011; Tost et al., 2006), applied from the surface to the top of the model domain, therefore enabling the consistent simulation of ozone transport from the stratosphere to the troposphere. A tracer for stratospheric ozone (denoted as O3s) is also employed in order to facilitate the investigation of stratospheric contribution to tropospheric ozone. The O3s tracer is given the model ozone values in the stratosphere and follows the transport and destruction processes of ozone in the troposphere. When (or if) O3s enters back in the stratosphere it is re-initialized at stratospheric values (Roelofs and Lelieveld, 1997).

3 Results

3.1 Middle troposphere summertime ozone maximum

The monthly average ozone fields at 500 hPa based on ERA-interim ozone over the period 1998–2009 (Fig. 2) show a latitudinal distribution of ozone with highest values towards the south for all months except from June to September. Specifically, in June an area with maximum ozone concentrations evolves over the EMME, which becomes more pronounced in July and August. This characteristic pool of high ozone values in the middle troposphere over the EMME is not solely a feature seen in the ERA-interim data but also in observed ozone data like the TES profiles. The daily TES ozone data were used to calculate the ozone anomalies in the middle troposphere (464 hPa) for July–August over the period 2005–2009 (Fig. 3b). Figure 3b shows the ozone anomalies for July–August at 450 hPa obtained from the ERA-interim data for the same period (2005–2009) and using the same days in accordance with TES data.

Inspection of both TES and ERA-interim ozone fields (Fig. 3) clearly corroborates the pool with high ozone values in middle troposphere over EMME.

3.2 Ozone links with circulation

The ERA-interim July–August average fields of ozone at 700 hPa (Fig. 4a) indicate that the pool with high ozone values extends geographically in the lower troposphere. Hence it appears that the enhanced ozone over the EMME is a robust feature, propagating down into the lower free troposphere. Inspection of the July–August ozone fields at 250 hPa (Fig. 4c) shows a structure of high ozone penetrating southwards over Southeastern Europe and the Eastern Mediterranean implying upper troposphere–lower troposphere links through meteorological processes.

It is well known that tropopause folding events at mid-latitudes are characterized by tongues of anomalously high potential vorticity (PV), high ozone, and low specific humidity (SH) (Holton et al., 1995). Both PV and SH are typical tracers to accompany ozone analysis in cases studies of transport from the lower stratosphere or upper troposphere into the middle and lower troposphere. It can be inferred from the comparison of Fig. 4a and b with Fig. 4d and e and Fig. 4g and h that the high ozone values in middle and lower troposphere are accompanied by structures of high PV and low SH. The similarities among the fields of ozone, PV and SH from the upper to lower troposphere imply the dominating role of transport for the high ozone values over the EMME. The high ozone, high PV and low SH over the EMME are related through the strong subsidence over the region as illustrated in Fig. 4i, k and l, showing the strong downward vertical velocities.

The penetration of dry air rich in ozone and PV from the upper troposphere/lower stratosphere to the lower troposphere is nicely illustrated from the latitude-altitude and longitude-altitude cross sections (centered over Crete) in Fig. 5. Specifically, the ERA-interim July–August latitude-altitude cross sections at a longitude of 24.5° E show a north–south descending structure of high ozone (Fig. 5a), high PV (Fig. 5c) and low SH (Fig. 5e) over the EMME. At the same time Fig. 5g shows clearly the strong subsidence with downward vertical velocities throughout most of the tropospheric column. It should be also noted in Fig. 5g that there is a lack of divergence for the largest part of the tropospheric column (zero divergence between 350 hPa and 800 hPa) with the air masses converging at the top (around 200–300 hPa) and diverging in the boundary layer (below 850 hPa), thus indicating limited outflow within the tropospheric column. Hence this large-scale subsidence over the region from the upper to lower troposphere accompanied by the limited outflow for the largest part of the tropospheric column accounts for the descending structures of ozone, PV and SH. Similarly, the respective longitude-altitude cross sections at a latitude of 35.25° N (Fig. 5b, d, f and h) illustrate the large scale transport mechanisms controlling atmospheric composition of Eastern Mediterranean (20° E to 40° E), in contrast to the Central and Western Mediterranean.

Hence, the links between ozone, potential vorticity and water vapour mixing ratios document that the dominant mechanism for the free tropospheric ozone pool is the downward transport from the upper troposphere and lower stratosphere, associated with enhanced subsidence and limited outflow (lack of divergence for the largest part of the tropospheric column) that dominate over the summertime EMME. It should be emphasized that the above mentioned ERA-interim results for the period 1998–2009 are robust and are the same for the extended time period 1979–2009.

3.3 EMAC results

The EMAC simulated July–August average ozone fields (1998–2009) in the middle (486 hPa) and lower free troposphere (714 hPa) are shown in Fig. 6a and b, respectively, and illustrate the pool with high ozone values over the EMME, in agreement with the ERA-interim results. To quantify the contribution of stratospheric ozone to these elevated tropospheric ozone values in the middle and lower free troposphere, the simulated in EMAC stratospheric ozone tracer (O3s) was investigated. The July–August average fields of the EMAC simulated O3s clearly illustrate (Fig. 6c) a structure of high values (up to 42 ppbv) in the middle troposphere over the Eastern Mediterranean and Minor Asia which actually also extend geographically to central Asia (east of the

Caspian Sea). This structure of high O3s values corresponds to around 40–45 % of the ozone in the middle troposphere. Furthermore, in the lower free troposphere (Fig. 6d) the EMAC simulations also clearly indicate a pool of high O3s over the EMME (up to around 26 ppbv) which corresponds to around 30–35 % of the ozone in the lower free troposphere. These results indicate the important contribution of stratospheric ozone to the pool of high ozone values over the EMME down to the lower free troposphere.

The downward transport of EMAC simulated ozone and the stratospheric ozone tracer from lower stratosphere/upper troposphere is further illustrated from the latitude-altitude and longitude-altitude cross sections in Fig. 7. The average July–August latitude-altitude cross sections at a longitude of 25° E show a north–south descending structure of high ozone (Fig. 7a) and O3s (Fig. 7b) from the upper into the lower tropospheric levels (down to 800 hPa), in agreement with the ERA-interim analysis (Fig. 5). A similar picture emerges from the respective longitude-altitude cross sections at a latitude of 35° N (Fig. 7c and d). Figure 7 also illustrates the different impacts of downward transport of the stratospheric ozone tracer between the Eastern and Central-Western Mediterranean. In general, the investigation of the EMAC simulations confirms the large contribution of stratospheric ozone to the pool of high ozone values over the EMME in the middle and lower free troposphere, in agreement with the ERA-interim analysis (see Sect 3.2).

3.4 Implications for the near surface ozone in Mediterranean

It was pointed out earlier that there is a difference between the Eastern and Central-Western Mediterranean concerning the downward transport of stratospheric ozone associated with the enhanced subsidence that dominates over the EMME. This leads to highest ozone in the middle and lower free troposphere over the EMME during summer, illustrated by ERA-interim, TES and EMAC data. Here we discuss the possible implications for the seasonal cycle of near surface ozone in the Mediterranean Basin. We selected four EMEP baseline maritime ozone stations along the Mediterranean Basin

(Fig. 1). From the EMAC simulated ozone and O3s data, the closest grid cells to the stations coordinates were selected.

The EMAC simulated ozone in the lower free troposphere (714 hPa) illustrates a summer maximum over the Eastern Mediterranean stations at Cyprus (CY02) and Crete (GR02) peaking in July–August and broad spring-summer maximum at Gozo, Malta (MT01) in Central Mediterranean and Cabo de Creus, Spain (ES10) in Western Mediterranean (Fig. 8a). The highest summertime values of ozone in the lower free troposphere simulated by the EMAC model are located over the most eastern station at Cyprus (Fig. 8a), confirming the enhanced subsidence in this region with respect to the Western and Central Mediterranean. This distinction in the seasonal cycle of the modelled lower free tropospheric ozone with higher values during summer over the EMME is due to the predominant contribution of stratospheric ozone (Fig. 8b). It should be noted from Fig. 8b that the O3s values in summer increase in easterly direction over the Mediterranean Basin. For example the lower free tropospheric O3s values in August at CY02 and GR02 are 13 ppbv and 8 ppbv higher than at MT01 and ES10, respectively. The above results indicate the ability of the EMAC model to reproduce spatial characteristics of the summertime ozone distribution in the lower free troposphere over the Mediterranean Basin (namely the spatial differences of Eastern Mediterranean vs. Central and Western Mediterranean).

However, near the surface the distinction of O3s among the four stations in summer months (Fig. 8d) becomes small (about 1.5 to 2 ppbv higher at CY02 and GR02 than at MT01 and ES10). Furthermore, the four stations show similarities in the shape of near surface modelled seasonal ozone cycle with a broad spring-summer maximum peaking in August (Fig. 8c). This result implies that photochemical processes dominate over downward transport processes in the seasonal ozone cycle in the Mediterranean boundary layer in EMAC simulations.

The observed near-surface ozone seasonal cycles at the four stations (Fig. 8e) show some similarities and some differences with the modelled ones. The EMAC model clearly overestimates ozone at all four stations during the summer months, typically by about 10 to 20 ppbv (20–35 %) as it is illustrated in Fig. 8f. This is attributed to overestimated photochemical ozone production in the boundary layer in the EMAC simulations during summer months. This is further illustrated by the larger amplitude of the seasonal cycle of near surface ozone in EMAC compared to observations and the fact that the model bias (modelled-observed near surface ozone monthly values) has a seasonal behaviour with the highest biases attained during summer (Fig. 8f). This discrepancy is related to the course horizontal grid resolution of the model version used (250–300 km), which artificially mixes ozone precursors, notably NO_x, over a large volume whereas in reality NO_x transport from pollution sources to these background stations is limited by its short atmospheric lifetime in summer. As a consequence, the fractional contribution by in situ produced ozone is over- and the contribution by O3s is underestimated. The course horizontal resolution of EMAC has been a compromise to allow high vertical resolution in the stratosphere and upper troposphere. Future work should consider increased horizontal resolution.

Nevertheless, the shape of the seasonal cycle, e.g. the observed near-surface ozone maximum at GR02 in July–August is reproduced by the model, while at CY02 there is a slight difference as it peaks in July (observations) rather than in July–August (model values). Over MT01 and ES10 there is a distinct ozone spring maximum in the observations, which is in better agreement with the modelled ozone cycle in the lower free troposphere (at 714 hPa) than at the surface. Again the discrepancy between observations and model at the surface is explained by the overestimated in EMAC photochemical ozone formation within the boundary layer, associated with long-distance transport of NO_x and other precursor gases from the polluted European continent toward the considered marine background stations, which masks the contribution of downward transport.

4 Discussion and conclusions

A 12 yr climatological analysis (1998–2009) of free tropospheric ozone was carried out based on ERA-interim reanalysis data and simulations with the EMAC atmospheric chemistry–climate model nudged towards ECMWF analysis data. A characteristic summertime pool with high ozone concentrations is found in the middle troposphere over the Eastern Mediterranean/Middle East (EMME) in the ERA-interim ozone data. This characteristic pool of high ozone in the middle troposphere over the EMME is also apparent from observed TES ozone profiles (2005–2009) and further supported by EMAC simulations. The EMAC model resolves adequately the region around the tropopause and it includes a stratospheric ozone tracer to facilitate the investigation of stratospheric contributions to tropospheric ozone.

The middle troposphere summertime ozone feature over the EMME area has been mentioned previously in a number of observational and modelling studies (e.g. Marenco et al., 1998; Stohl et al., 2001; Jonson et al., 2001; Li et al., 2001; Roelofs et al., 2003). The analysis of ERA-interim data and EMAC results corroborate that the enhanced ozone over the EMME is a robust feature, propagating downward to lower free tropospheric levels.

The links of ozone with other transport tracers such as potential vorticity and water vapour indicate that the dominant mechanism for the free tropospheric ozone pool is downward transport from the upper troposphere and lower stratosphere associated with the enhanced subsidence and limited outflow that characterize the summertime EMME circulation. Furthermore the EMAC simulations indicate the large contribution of stratospheric ozone to the pool of high ozone values over EMME in the middle and lower free troposphere. Traub and Lelieveld (2003) investigated cross-tropopause transport over the Eastern Mediterranean by analyzing trajectories for the MINOS campaign and found from analysis of the residence times in stratosphere and troposphere after crossing the tropopause (set at 3.5 PVU), that the transport is vertically shallow and that this mixing of tropospheric and stratospheric air is largely confined to the tropopause region during summer.

Taking into account the results of Traub and Lelieveld (2003) we infer that shallow STT processes feed stratospheric ozone into the upper troposphere, and subsequently these air masses (rich in ozone) are transported to lower free tropospheric levels through the characteristic strong summertime EMME subsidence and the limited outflow. Nevertheless, the contribution of deep STT events should not be disregarded since the Eastern Mediterranean is a region favorable to deep STT events (Sprenger and Wernli, 2003), though these events preferentially develop from the North Atlantic sector. Our results are in agreement with the findings of Kalabokas et al. (2007, 2013) who concluded that the highest ozone concentrations in the lower troposphere over the Eastern Mediterranean and subsequently in the boundary layer are associated with large scale subsidence of ozone rich air masses from the upper troposphere. They are also in agreement with Roelofs et al. (2003) who showed substantial contributions to elevated ozone in the middle troposphere by transport from the stratosphere. Furthermore, our findings are partially in line with the study of Li et al. (2001) who concluded that large-scale subsidence over the region with continued net production of ozone and little mid-level outflow is a major mechanism, but in contrast to our results they deduced that transport from the stratosphere does not contribute significantly to the ozone maximum. This substantiates the need to apply a model that realistically simulates stratosphere–troposphere exchange processes (in the present work at the expense of horizontal resolution near the surface).

The differences in the seasonal cycle of the modelled lower free tropospheric ozone across the Mediterranean Basin (with highest values during summer towards the east) indicates the ability of the EMAC model to reproduce notable spatial characteristics of the ozone distribution in the lower free troposphere over the region. This is a consequence of the emphasis of the selected EMAC version to accurately reproduce the dynamical processes around the tropopause. In support of this, it should be noted that simulations with a regional air quality model (CAMx) showed an underestimation of surface ozone during summer at baseline stations in the Eastern Mediterranean due to the limited vertical domain (top at around 6 km) and hence the lack of realistic middle tropospheric conditions to simulate the effects of subsidence on near surface ozone (Akritidis et al., 2013).

However, within the atmospheric boundary layer long-distance pollution transport and photochemical processes dominate over downward ozone transport in EMAC simulations. The overestimate of NO_x and other ozone precursor transport from the European continent due to the coarse horizontal resolution of the EMAC model leads to a rather spatially uniform seasonal ozone cycle over the Mediterranean Basin. This result is not supported by the EMEP observations which show a seasonal cycle peaking in summer for Eastern Mediterranean stations and a seasonal cycle peaking in spring for Central and Western Mediterranean stations (Fig. 8e). The discrepancy between EMAC and observed ozone near the surface is attributed to overestimated modelled photochemical ozone production during summer related to the course horizontal resolution thus partially masking the contribution of downward transport which is stronger over Eastern Mediterranean than over Central and Western Mediterranean. Furthermore, it is important to accurately resolve boundary layer processes because the representation of entrainment from the lower free troposphere is expected to be important as well. For example, Gerasopoulos et al. (2006) based on observations showed that the dominating factor for the maximum ozone values during summer at Finokalia station is the entrainment of ozone rich air masses from the free troposphere.

Therefore, it is suggested that model studies focusing on tropospheric ozone over the EMME region should realistically represent both stratosphere-troposphere exchange processes and boundary layer transport and photochemistry at high horizontal and vertical resolution.

Acknowledgements. The research leading to these results has received funding from the European Research Council under the European Union's Seventh Framework Programme (FP7/2007-2013)/ERC grant agreement no. 226144. Part of the study was supported by IKY in the framework of the Greece–Germany Exchange and Cooperation Programme, IKYDA 2012.

References

Akritidis, D., Zanis, P., Pytharoulis, I., Mavrakis, A., and Karacostas, T.: A deep stratospheric intrusion event down to the earth's surface of the megacity of Athens, Meteorol. Atmos. Phys., 109, 9–18, doi:10.1007/s00703-010-0096-6, 2010.

Akritidis, D., Zanis, P., Katragkou, E., Schultz, M., Tegoulias, I., Poupkou, A., Markakis, K., Pytharoulis, I., and Karacostas, T.: Evaluation of near surface ozone in RegCM3/CAMx simulations over Europe for the period 1996–2000: the impact of chemical boundary conditions, Atmos. Res., doi:10.1016/j.atmosres.2013.07.021, in press, 2013.

Anagnostopoulou, C., Zanis, P., Katragkou, E., Tegoulias, I., and Tolika, K.: Recent past and future patterns of the Etesian winds based on regional scale climate model simulations, Clim. Dynam., accepted, 2013.

Beer, R.: TES on the Aura Mission: scientific objectives, measurements and analysis overview, IEEE T. Geosci. Remote, 44, 1102–1105, 2006.

Beer, R., Glavich, T. A., and Rider, D. M.: Tropospheric emission spectrometer for the Earth observing system's Aura satellite, Appl. Optics, 40, 2356–2367, 2001.

Berrisford, P., Dee, D., Fielding, K., Fuentes, M., Kållberg, P., Kobayashi, S., and Uppala, S.: The ERA-Interim Archive, ERA Report Series, 1. Technical Report, European Centre for Medium-Range Weather Forecasts, Shinfield Park, Reading, 16 pp., 2009.

Berrisford, P., Kållberg, P., Kobayashi, S., Dee, D., Uppala, S., Simmons, A. J., Poli, P., and Sato, H.: Atmospheric conservation properties in ERA-Interim, Q. J. Roy. Meteor. Soc., 137, 1381–1399, doi:10.1002/qj.864, 2011.

Cariolle, D. and Déqué, M.: Southern Hemisphere medium-scale waves and total ozone disturbances in a spectral general circulation model, J. Geophys. Res., 91, 10825–10846, 1986.

Cariolle, D. and Teyssèdre, H.: A revised linear ozone photochemistry parameterization for use in transport and general circulation models: multi-annual simulations, Atmos. Chem. Phys., 7, 2183–2196, doi:10.5194/acp-7-2183-2007, 2007.

Chameides, W. and Walker, J. C. G.: A photochemical theory of tropospheric ozone, J. Geophys. Res., 78, 8751–8760, 1973.

Crutzen, P. J.: Tropospheric ozone: an overview, in: Tropospheric Ozone, edited by: Isaksen, I. S. A., D. Reidel Publ. Co., 3–32, 1988.

Crutzen, P. J., Lawrence, M. G., and Pöschl, U.: On the background photochemistry of tropospheric ozone, Tellus A, 51, 123–146, 1999.

Dee, D. P., Uppala, S. M., Simmons, A. J., Berrisford, P., Poli, P., Kobayashi, S., Andrae, U., Balmaseda, M. A., Balsamo, G., Bauer, P., Bechtold, P., Beljaars, A. C. M., van de Berg, L., Bidlot, J., Bormann, N., Delsol, C., Dragani, R., Fuentes, M., Geer, A. J., Haimberger, L., Healy, S. B., Hersbach, H., Hólm, E. V., Isaksen, L., Kållberg, P., Köhler, M., Matricardi, M., McNally, A. P., Monge-Sanz, B. M., Morcrette, J.-J., Park, B.-K., Peubey, C., de Rosnay, P., Tavolato, C., Thépaut, J.-N., and Vitart, F.: The ERA-Interim reanalysis: configuration and performance of the data assimilation system, Q. J. Roy. Meteor. Soc., 137, 553–597, doi:10.1002/qj.828, 2011.

Dethof, A. and Hólm, E.: Ozone assimilation in the ERA-40 reanalysis project, Q. J. Roy. Meteor. Soc.,130, 2851–2872, 2004.

Dragani, R.: On the quality of the ERA-Interim ozone reanalyses: comparisons with satellite data, Q. J. Roy. Meteor. Soc., 137, 1312–1326, doi:10.1002/qj.821, 2011.

Galani, E., Balis, D., Zanis, P., Zerefos, C., Papayannis, A., Wernli, H., and Gerasopoulos, E.: Observations of stratosphere-troposphere transport events over the eastern Mediterranean using a ground-based lidar system, J. Geophys. Res., 108, D128527, doi:10.1029/2002JD002596, 2003.

Gerasopoulos, E., Kouvarakis, G., Vrekoussis, M., Kanakidou, M., and Mihalopoulos, N.: Ozone variability in the marine boundary layer of the Eastern Mediterranean based on 7-year observations, J. Geophys. Res., 110, D15309, doi:10.1029/2005JD005991, 2005.

Gerasopoulos, E., Kouvarakis, G., Vrekoussis, M., Donoussis, C., Mihalopoulos, N., and Kanakidou, M.: Photochemical ozone production in the Eastern Mediterranean, Atmos. Environ., 40, 3057–3069, doi:10.1016/j.atmosenv.2005.12.061, 2006.

Holton, J. R., Haynes, P. H., McIntyre, E. M., Douglass, A. R., Rood, R. B., and Pfister, L.: Stratosphere-troposphere exchange, Rev. Geophys., 33, 403–439, 1995.

Im, U., Markakis, K., Poupkou, A., Melas, D., Unal, A., Gerasopoulos, E., Daskalakis, N., Kindap, T., and Kanakidou, M.: The impact of temperature changes on summer time ozone and its precursors in the Eastern Mediterranean, Atmos. Chem. Phys., 11, 3847–3864, doi:10.5194/acp-11-3847-2011, 2011.

IPCC: Climate Change 2007, The Physical Science Basis, Contribution of Working Group I to the Fourth Assessment Report of the Intergovernmental Panel on Climate Change, edited by: Solomon, S., Qin, D., Manning, M., Chen, Z., Marquis, M., Averyt, K. B., Tignor, M., and Miller, H. L., Cambridge University Press, Cambridge, UK and New York, NY, USA, 996 pp., 2007.

Jöckel, P., Sander, R., Kerkweg, A., Tost, H., and Lelieveld, J.: Technical Note: The Modular Earth Submodel System (MESSy) – a new approach towards Earth System Modeling, Atmos. Chem. Phys., 5, 433–444, doi:10.5194/acp-5-433-2005, 2005.

Jöckel, P., Tost, H., Pozzer, A., Brühl, C., Buchholz, J., Ganzeveld, L., Hoor, P., Kerkweg, A., Lawrence, M. G., Sander, R., Steil, B., Stiller, G., Tanarhte, M., Taraborrelli, D., van Aardenne, J., and Lelieveld, J.: The atmospheric chemistry general circulation model ECHAM5/MESSy1: consistent simulation of ozone from the surface to the mesosphere, Atmos. Chem. Phys., 6, 5067–5104, doi:10.5194/acp-6-5067-2006, 2006.

Jöckel, P., Kerkweg, A., Pozzer, A., Sander, R., Tost, H., Riede, H., Baumgaertner, A., Gromov, S., and Kern, B.: Development cycle 2 of the Modular Earth Submodel System (MESSy2), Geosci. Model Dev., 3, 717–752, doi:10.5194/gmd-3-717-2010, 2010.

Jonson, J. E., Sunder, J. K., and Tarrasón, L.: Model calculations of present and future levels of ozone and ozone precursors with a global and a regional model, Atmos. Environ., 35, 525–537, 2001.

Kalabokas, P. D. and Bartzis, J. G.: Photochemical air pollution characteristics at the station of the NCSR-Demokritos, during the MEDCAPHOT-TRACE campaign, Greece (20 August–20 September 1994), Atmos. Environ., 32, 2123–2139, 1998.

Kalabokas, P. D. and Repapis, C. C.: A climatological study of rural surface ozone in central Greece, Atmos. Chem. Phys., 4, 1139–1147, doi:10.5194/acp-4-1139-2004, 2004.

Kalabokas, P. D., Viras, L. G., Bartzis, J. G., and Repapis, C. C.: Mediterranean rural ozone characteristics around the urban area of Athens, Atmos. Environ., 34, 5199–5208, 2000.

Kalabokas, P. D., Volz-Thomas, A., Brioude, J., Thouret, V., Cammas, J.-P., and Repapis, C. C.: Vertical ozone measurements in the troposphere over the Eastern Mediterranean and comparison with Central Europe, Atmos. Chem. Phys., 7, 3783–3790, doi:10.5194/acp-7-3783-2007, 2007.

Kalabokas, P. D., Mihalopoulos, N., Ellul, R., Kleanthous, S., and Repapis, C. C.: An investigation of the meteorological and photochemical factors influencing the background rural and marine surface ozone levels in the Central and Eastern Mediterranean, Atmos. Environ., 42, 7894–7906, 2008.

Kalabokas, P. D., Cammas, J.-P., Thouret, V., Volz-Thomas, A., Boulanger, D., and Repapis, C. C.: Examination of the atmospheric conditions associated with high and low summer ozone levels in the lower troposphere over the Eastern Mediterranean, Atmos. Chem. Phys. Discuss., 13, 2457–2491, doi:10.5194/acpd-13-2457-2013, 2013.

Kallos, G., Kotroni, V., Lagouvardos, K., and Papadopoulos, A.: On the long range transport of air pollutants from Europe to Africa, Geophys. Res. Lett., 25, 619–622, 1998.

Kanakidou, M., Mihalopoulos, N., Kindap, T., Im, U., Vrekoussis, M., Gerasopoulos, E., Dermitzaki, E., Unal, A., Koçak, M., Markakis, K., Melas, D., Kouvarakis, G., Youssef, A. F., Richter, A., Hatzianastassiou, N., Hilboll, A., Ebojie, F., Wittrock, F., von Savigny, C., Burrows, J. P., Ladstaetter-Weissenmayer, A., and Moubasher, H.: Megacities as hot spots of air pollution in the East Mediterranean, Atmos. Environ., 45, 1223–1235, doi:10.1016/j.atmosenv.2010.11.048, 2011.

Kourtidis, K., Ziomas, I., Zerefos, C., Balis, D., Suppan, P., Vassaras, A., Kosmidis, V., and Kentarchos, A.: On the background ozone values in Greece, Seventh European Symposium on Physico-chemical Behaviour of Atmospheric Pollutants: the Oxidizing Capacity of the Troposphere, EUR 17482 EN, Venice, Italy, 456–461, 1996.

Kourtidis, K., Zerefos, C., Rapsomanikis, S., Simeonov, V., Balis, D., Perros, P. E., Thomson, A. M., Witte, J., Calpini, B., Sharobiem, W. M., Papayiannis, A., Mihalopoulos, N., and Drakou, R.: Regional levels of ozone in the troposphere over Eastern Mediterranean, J. Geophys. Res., 107, 8140, doi:10.1029/2000JD000140, 2002.

Kouvarakis, G., Tsigaridis, K., Kanakidou, M., and Mihalopoulos, N.: Temporal variations of surface regional background ozone over Crete Island in the southeast Mediterranean, J. Geophys. Res., 105, 4399–4407, 2000.

Kouvarakis, G., Vrekoussis, M., Mihalopoulos, N., Kourtidis, K., Rappenglueck, B., Gerasopoulos, E., and Zerefos, C.: Spatial and temporal variability of tropospheric ozone in the boundary layer above the Aegean Sea (Eastern Mediterranean), J. Geophys. Res., 107, 8137, doi:10.1029/2000JD000081, 2002.

Lacis, A. A., Wuebbles, D. J., and Logan, J. A.: Radiative forcing of climate by changes in the vertical distribution of ozone, J. Geophys. Res., 95, 9971–9981, 1990.

Lelieveld, J. and Dentener, F. J.: What controls tropospheric ozone?, J. Geophys. Res., 105, 3531–3551, 2000.

Lelieveld, J., Berresheim, H., Borrmann, S., Crutzen, P. J., Dentener, F. J., Fischer, H., de Gouw, J., Feichter, J., Flatau, P., Heland, J., Holzinger, R., Korrmann, R., Lawrence, M., Levin, Z., Markowicz, K., Mihalopoulos, N., Minikin, A., Ramanathan, V., de Reus, M., Roelofs, G.-J., Scheeren, H. A., Sciare, J., Schlager, H., Schultz, M., Siegmund, P., Steil, B., Stephanou, E., Stier, P., Traub, M., Williams, J., and Ziereis, H.: Global air pollution crossroads over the Mediterranean, Science, 298, 794–799, 2002.

Lelieveld, J., Brühl, C., Jöckel, P., Steil, B., Crutzen, P. J., Fischer, H., Giorgetta, M. A., Hoor, P., Lawrence, M. G., Sausen, R., and Tost, H.: Stratospheric dryness: model simulations and satellite observations, Atmos. Chem. Phys., 7, 1313–1332, doi:10.5194/acp-7-1313-2007, 2007.

Lelieveld, J., Hoor, P., Jöckel, P., Pozzer, A., Hadjinicolaou, P., Cammas, J.-P., and Beirle, S.: Severe ozone air pollution in the Persian Gulf region, Atmos. Chem. Phys., 9, 1393–1406, doi:10.5194/acp-9-1393-2009, 2009.

Li, Q., Jacob, D. J., Logan, J. A., Bey, I., Yantosca, R. M., Liu, H., Martin, R. V., Fiore, A. M., Field, B. D., Duncan, B. N., and Thouret, V.: A tropospheric ozone maximum over the Middle East, Geophys. Res. Lett., 28, 3235–3238, doi:10.1029/2001GL013134, 2001.

Liakakou, E., Vrekoussis, M., Bonsang, B., Donousis, C., Kanakidou, M., and Mihalopoulos, N.: Isoprene above the Eastern Mediterranean: seasonal variation and contributionto the oxidation capacity of the atmosphere, Atmos. Environ., 41, 1002–1010, doi:10.1016/j.atmosenv.2006.09.034, 2007.

Marenco, A., Thouret, V., Nédélec, P., Smit, H. G. J., Helten, M., Kley, D., Karcher, F., Simon, P., Law, K., Pyle, J., Poschmann, G., Von Wrede, R., Hume, C., and Cook, T.: Measurement of ozone and water vapor by Airbus in-service aircraft: the MOZAIC airborne program, an overview, J. Geophys. Res., 103, 25631–25642, doi:10.1029/98JD00977, 1998.

Penkett, S. A.: Indications and causes of ozone increase in the troposphere, in: The Changing Atmosphere, edited by: Rowland, F. S. and Isaksen, I. S. A., J. Wiley & Sons, 91 pp., 1988.

Poupkou, A., Zanis, P., Nastos, P., Papanastasiou, D., Melas, D., Tourpali, K., and Zerefos, C.:Present climate trend analysis of the Etesian winds in the Aegean Sea, Theor. Appl. Climatol., 106, 459–472, doi:10.1007/s00704-011-0443-7, 2011.

Pozzer, A., Jöckel, P., Tost, H., Sander, R., Ganzeveld, L., Kerkweg, A., and Lelieveld, J.: Simulating organic species with the global atmospheric chemistry general circulation model ECHAM5/MESSy1: a comparison of model results with observations, Atmos. Chem. Phys., 7, 2527–2550, doi:10.5194/acp-7-2527-2007, 2007.

Repapis, C., Zerefos, C., and Tritakis, B.: On the Etesians over the Aegean, Proc. Acad. Athens, 52, 572–606, 1977.

Richards, N. A. D., Arnold, S. R., Chipperfield, M. P., Miles, G., Rap, A., Siddans, R., Monks, S. A., and Hollaway, M. J.: The Mediterranean summertime ozone maximum: global emission sensitivities and radiative impacts, Atmos. Chem. Phys., 13, 2331–2345, doi:10.5194/acp-13-2331-2013, 2013.

Rodwell, M. J. and Hoskins, B. J.: Monsoons and the dynamics of deserts, Q. J. Roy. Meteor. Soc., 122, 1385–1404, 1996.

Rodwell, M. J. and Hoskins, B. J.: Subtropical anticyclones and summer monsoons, J. Climate, 14, 3192–3211, 2001.

Roeckner, E., Brokopf, R., Esch, M., Giorgetta, M., Hagemann, S., Kornbluh, Manzini, L. E., Schlese, U., and Schulzweida, U.: Sensitivity of simulated climate to horizontal and vertical resolution in the ECHAM5 atmosphere model, J. Climate, 19, 3771–3791, 2006.

Roelofs, G. J. and Lelieveld, J.: Model study of the influence of cross-tropopause O_3 transports on tropospheric O_3 levels, Tellus B, 49, 38–55, 1997.

Roelofs, G. J., Scheeren, H. A., Heland, J., Ziereis, H., and Lelieveld, J.: A model study of ozone in the Eastern Mediterranean free troposphere during MINOS (August 2001), Atmos. Chem. Phys., 3, 1199–1210, doi:10.5194/acp-3-1199-2003, 2003.

Sander, R., Baumgaertner, A., Gromov, S., Harder, H., Jöckel, P., Kerkweg, A., Kubistin, D., Regelin, E., Riede, H., Sandu, A., Taraborrelli, D., Tost, H., and Xie, Z.-Q.: The atmospheric chemistry box model CAABA/MECCA-3.0, Geosci. Model Dev., 4, 373–380, doi:10.5194/gmd-4-373-2011, 2011.

Scheeren, H. A., Lelieveld, J., Roelofs, G. J., Williams, J., Fischer, H., de Reus, M., de Gouw, J. A., Warneke, C., Holzinger, R., Schlager, H., Klüpfel, T., Bolder, M., van der Veen, C., and Lawrence, M.: The impact of monsoon outflow from India and Southeast Asia in the upper troposphere over the Eastern Mediterranean, Atmos. Chem. Phys., 3, 1589–1608, doi:10.5194/acp-3-1589-2003, 2003.

Sprenger, M. and Wernli, H.: A northern hemispheric climatology of cross-tropopause exchange for the ERA15 time period (1979–1993), J. Geophys. Res., 108, D128521, doi:10.1029/2002JD002636, 2003.

Stohl, A., James, P., Forster, C., Spichtinger, N., Marenco, A., Thouret, V., and Smit, H. G. J.: An extension of MOZAIC ozone climatologies using trajectory statistics, J. Geophys. Res., 106, 27757–27768, 2001.

Tost, H., Jöckel, P., Kerkweg, A., Sander, R., and Lelieveld, J.: Technical note: A new comprehensive SCAVenging submodel for global atmospheric chemistry modelling, Atmos. Chem. Phys., 6, 565–574, doi:10.5194/acp-6-565-2006, 2006.

Traub, M. and Lelieveld, J.: Cross-tropopause transport over the Eastern Mediterranean, J. Geophys. Res., 108, D234712, doi:10.1029/2003JD003754, 2003.

Tyrlis, E. and Lelieveld, J.: Climatology and dynamics of the summer Etesian winds over the Eastern Mediterranean, J. Atmos. Sci., doi:10.1175/JAS-D-13-035.1, in press, 2013.

Tyrlis, E., Lelieveld, J., and Steil, B.: The summer circulation in the eastern Mediterranean and the Middle East: influence of the South Asian Monsoon, Clim. Dynam., 40, 1103–1123, doi:10.1007/s00382-012-1528-4, 2012.

Zerefos, C. S., Kourtidis, K. A., Melas, D., Balis, D., Zanis, P., Katsaros, L., Mantis, H. T., Repapis, C., Isaksen, I., Sundet, J., Herman, J,. Bhartia, P. K., and Calpini, B.: Photochemical Activity and Solar Ultraviolet Radiation (PAUR) modulation factors: an overview of the project, J. Geophys. Res., 107, 8134, doi:10.1029/2000JD000134, 2002.

Ziv, B., Saaroni, H., Alpert, P.: The factors governing the summer regime of the Eastern Mediterranean, Int. J. Climatol., 24, 1859–1871, 2004.

Fig. 1. Map of the Mediterranean Basin with the locations of the 4 EMEP stations marked: Cabo de Creus, Spain (ES10), Gozo, Malta (MT01), Finokalia, Greece (GR02) and Ag. Marina, Cyprus (CY02). Mind that the positions of the cross sections of Figs. 5 and 7 are indicated in the map by the 35° N meridian and the 25° E parallel crossing the island of Crete, Greece.

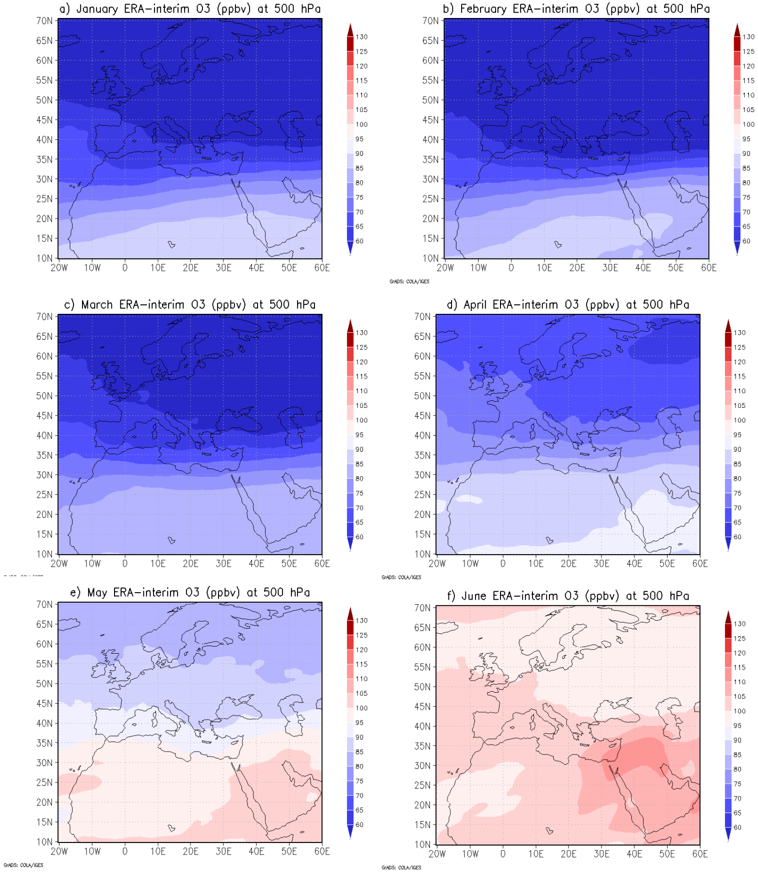

Fig. 2. Monthly average ozone fields at 500 hPa based on ERA-interim ozone (ppbv) over the period 1998–2009 for **(a)** January, **(b)** February, **(c)** March, **(d)** April, **(e)** May, **(f)** June, **(g)** July, **(h)** August, **(i)** September, **(j)** October, **(k)** November, **(l)** December.

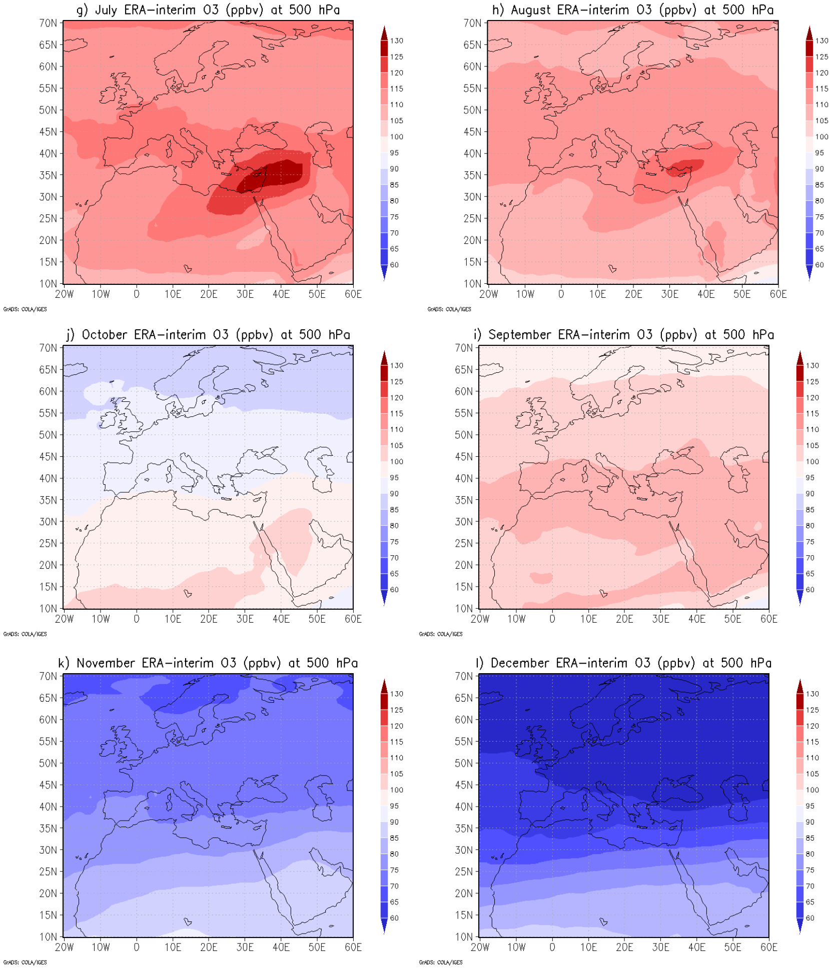

Fig. 2. Continued.

ACPD

13, 22025–22058, 2013

Summertime free tropospheric ozone over Mediterranean/ Middle East

P. Zanis et al.

Title Page
Abstract | Introduction
Conclusions | References
Tables | Figures
◄◄ | ►►
◄ | ►
Back | Close
Full Screen / Esc
Printer-friendly Version
Interactive Discussion

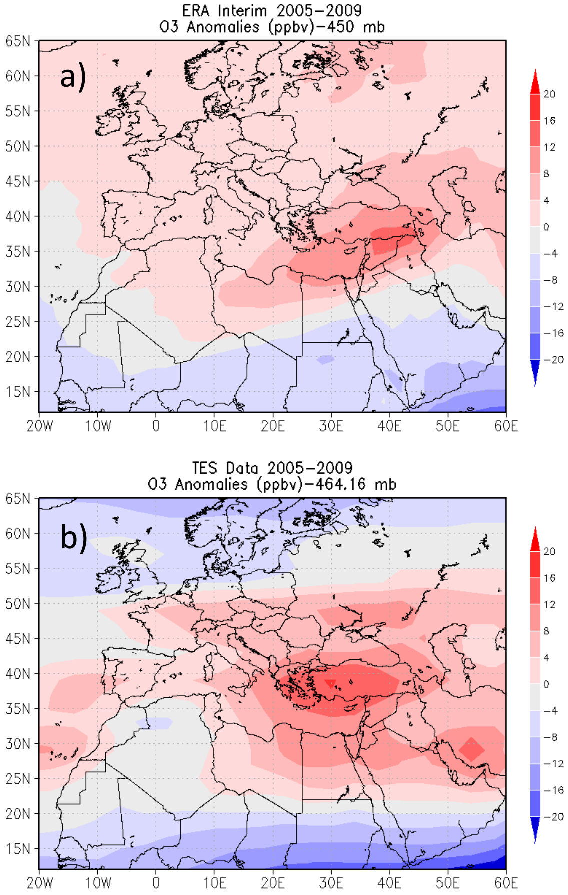

Fig. 3. July–August average ozone anomaly fields (ppbv) over the period 2005–2009 based on **(a)** ERA-interim ozone at 450 hPa, and on **(b)** TES observed ozone at 464 mb. Ozone anomalies were calculated as the differences between the July–August mean at each grid point and the July–August mean of the whole area of the domain.

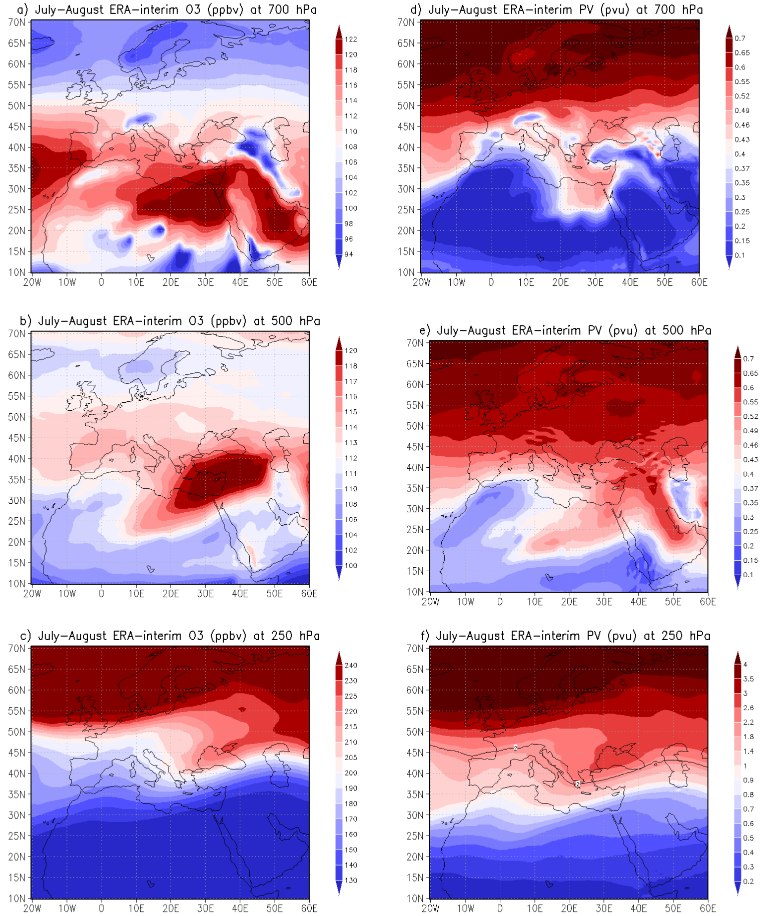

Fig. 4. ERA-interim July–August average fields of ozone (ppbv), potential vorticity (pvu), specific humidity (g kg^{-1}) and vertical velocity (Pa s^{-1}) over the period 1998–2009 at 700 hPa **(a, d, g, j)**, at 500 hPa **(b, e, h, k)** and at 250 hPa **(c, f, i, l)**, respectively.

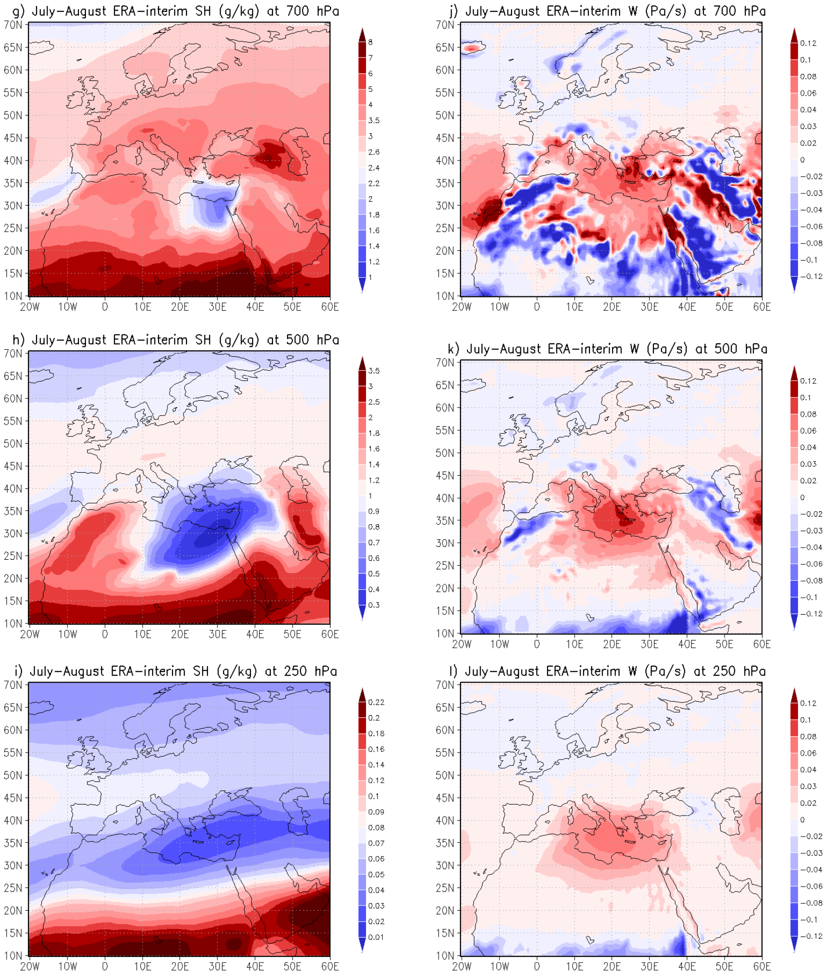
g) July–August ERA-interim SH (g/kg) at 700 hPa

j) July–August ERA-interim W (Pa/s) at 700 hPa

h) July–August ERA-interim SH (g/kg) at 500 hPa

k) July–August ERA-interim W (Pa/s) at 500 hPa

i) July–August ERA-interim SH (g/kg) at 250 hPa

l) July–August ERA-interim W (Pa/s) at 250 hPa

Fig. 4. Continued.

Title Page
Abstract
Introduction
Conclusions
References
Tables
Figures
◀◀
▶▶
◀
▶
Back
Close
Full Screen / Esc
Printer-friendly Version
Interactive Discussion

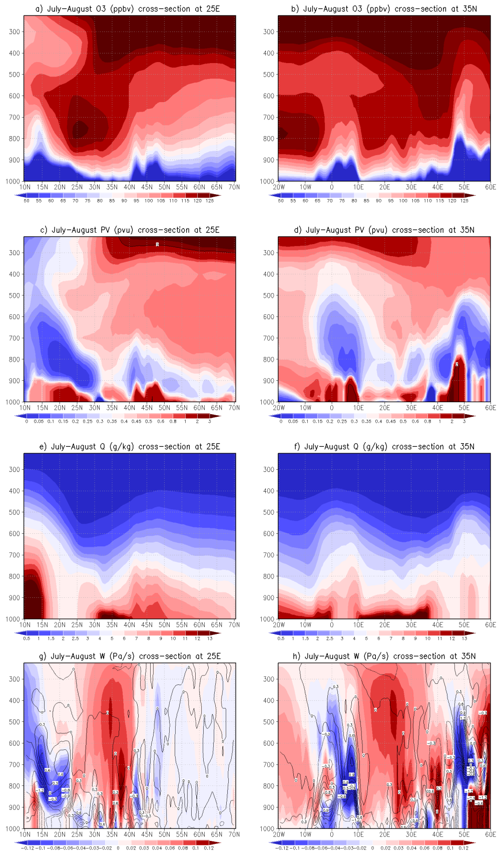

a) July–August O3 (ppbv) cross-section at 25E

b) July–August O3 (ppbv) cross-section at 35N

c) July–August PV (pvu) cross-section at 25E

d) July–August PV (pvu) cross-section at 35N

e) July–August Q (g/kg) cross-section at 25E

f) July–August Q (g/kg) cross-section at 35N

g) July–August W (Pa/s) cross-section at 25E

h) July–August W (Pa/s) cross-section at 35N

Fig. 5. Left column: ERA-interim July–August latitude-altitude cross sections at longitude 24.5° E of **(a)** ozone (ppbv), **(c)** potential vorticity (pvu), **(e)** specific humidity (g kg^{-1}) and **(g)** vertical velocity (Pa s^{-1}) averaged over the period 1998–2009. Right column: ERA-interim July–August longitude-altitude cross sections at 35.25° N latitude of **(b)** ozone (ppbv), **(d)** potential vorticity (pvu), **(f)** specific humidity (g kg^{-1}) and **(h)** vertical velocity (Pa s^{-1}) averaged over the period 1998–2009. The solid black line in **(c)** denotes the dynamical tropopause at 2 pvu. The contour lines in **(g)** and **(h)** denote the respective average values of divergence (s^{-1}).

Title Page
Abstract
Introduction
Conclusions
References
Tables
Figures
I◀
▶I
◀
▶
Back
Close
Full Screen / Esc
Printer-friendly Version
Interactive Discussion

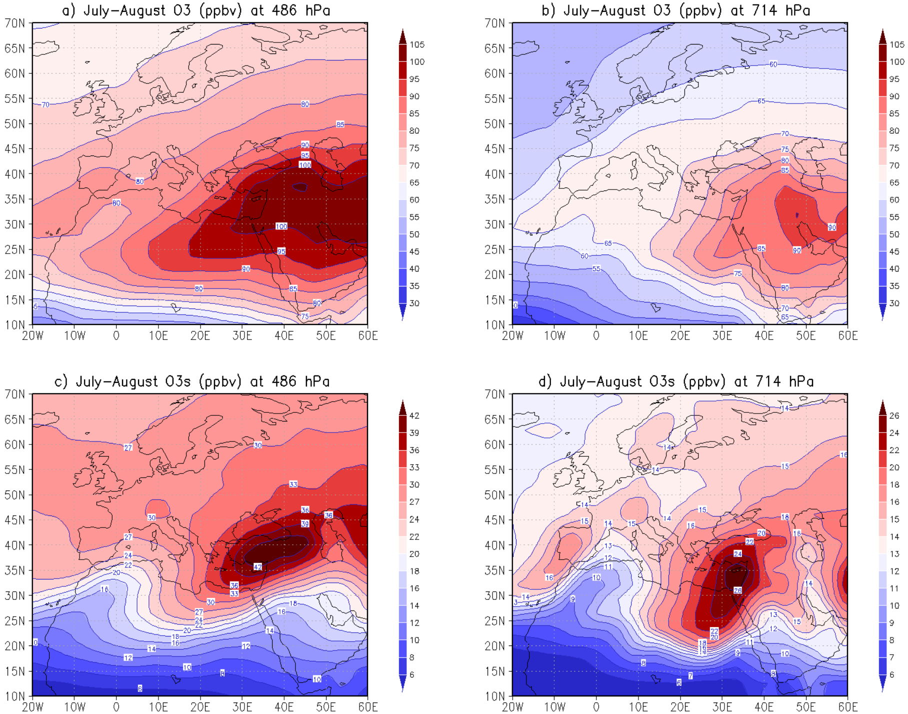

Fig. 6. EMAC July–August average fields of simulated ozone (ppbv) and the stratospheric ozone tracer O3s (ppbv) over the period 1998–2009 at 486 hPa **(a, c)** and at 714 hPa **(b, d)**, respectively.

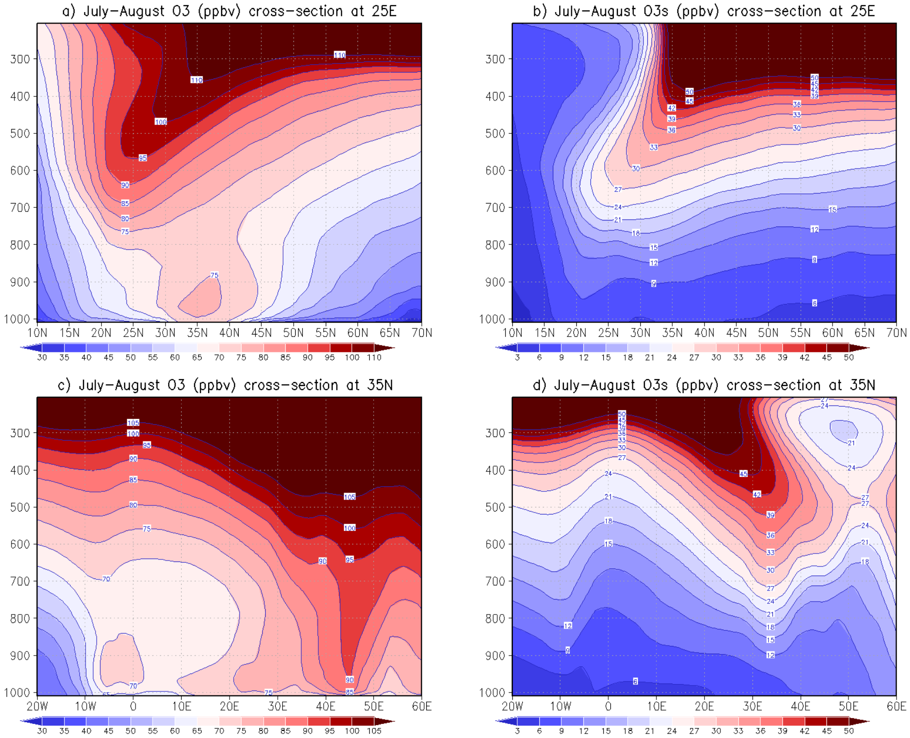

Fig. 7. Upper plates: EMAC July–August latitude-altitude cross sections at 25° E longitude of simulated **(a)** ozone (ppbv) and **(b)** stratospheric ozone tracer O3s (ppbv) averaged over the period 1998–2009. Bottom plates: EMAC July–August longitude-altitude cross sections at 35° N latitude of **(c)** ozone (ppbv) and **(d)** stratospheric ozone tracer (ppbv) averaged over the period 1998–2009.

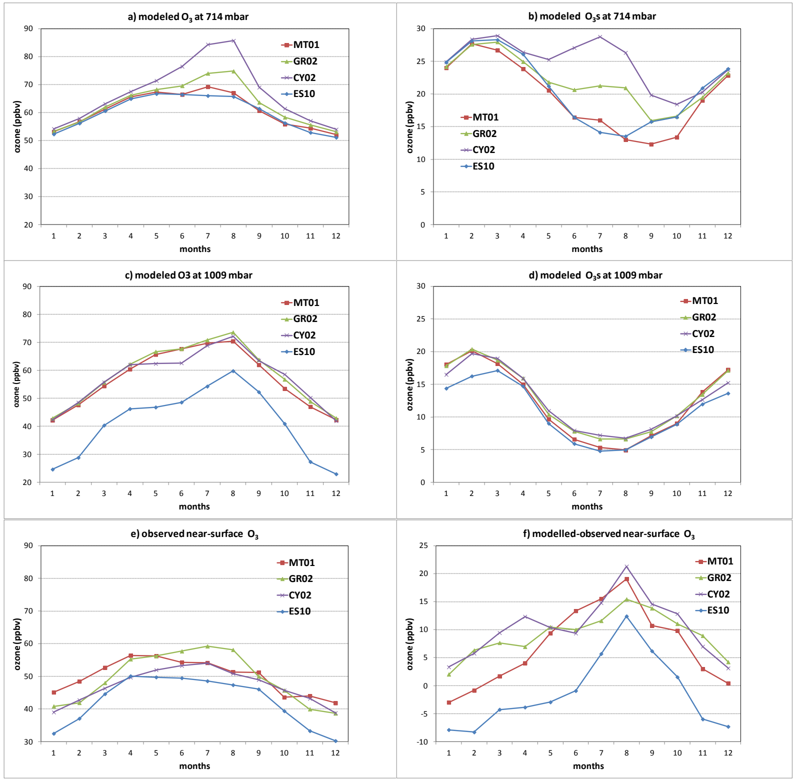

Fig. 8. Mean seasonal cycle over the period 1998–2008 of EMAC simulated ozone (ppbv) and stratospheric ozone tracer O3s (ppbv) at 714 hPa **(a, b)** and at 1009 hPa **(c, d)** as well as observed near surface ozone **(e)** and the difference between modelled and observed near surface ozone values **(f)** at the stations Gozo, Malta (MT01, red), Finokalia, Greece (GR02, green), Ag. Marina, Cyprus (CY02, purple) and Cabo de Creus, Spain (ES10, light blue). For the EMAC simulated data the closest grid cell to the station coordinates was selected.